

Characteristics of Probe Electrospray Generated from a Solid Needle

Lee Chuin Chen,[†] Kentaro Nishidate,[†] Yuta Saito,[†] Kunihiro Mori,[†] Daiki Asakawa,[†] Sen Takeda,^{‡,||} Takeo Kubota,^{§,||} Hirokazu Hori,^{||} and Kenzo Hiraoka^{*,†}

Clean Energy Research Center, University of Yamanashi, Takeda 4-3-11, Kofu 400-8511, Japan, Department of Anatomy and Cell Biology and Department of Epigenetic Medicine, Faculty of Medicine, University of Yamanashi, Shimo-Kateau 1110, Chuo, 409-3898, Japan, and Interdisciplinary Graduate School of Medicine and Engineering, University of Yamanashi, Takeda 4-3-11, Kofu 400-8511, Japan

Received: April 29, 2008; Revised Manuscript Received: June 10, 2008

Probe electrospray ionization (PESI) has recently been developed, in which the electrospray was generated from a solid needle instead of by using a capillary. In this paper, the characteristics of probe electrospray ionization were studied based on the measurement of spray current, optical microscopy, and PESI mass spectrometry. In the experiment, the solid needle was moved up and down a vertical axis, and a small amount of sample was repeatedly loaded to the needle when the tip of the needle touched the surface of the liquid sample at the lowest position. After the application of high voltage, a liquid droplet was formed on the tip of the solid needle probe, with its size was determined by the size of the needle tip. The liquid flow rate to the tip, as indicated by the spray current, depends on the voltage applied to the needle as well as the loaded liquid amount. Stable electrospray can be maintained until the total consumption of liquid sample. The kilohertz current pulsation takes place in the case of overloading the sample to the needle. The influences of the applied voltage and the liquid flow rate on the PESI mass spectra were also examined.

Introduction

In 1917, Zeleny observed the electrospray of liquid glycerin from a capillary,¹ and the electrified liquid meniscus, which took the shape of a cone, was theoretically analyzed by Taylor.² Dole et al. described that the molecular ions might be liberated from the electrospayed droplet,³ and the first electrospray ionization mass spectrometry (ESI-MS) was demonstrated by Fenn et al.^{4,5} ESI-MS has now become one of the indispensable tools for the analysis of biomolecules. Conventional electrospray generally employs a continuous-flow technique, where the liquid sample is pumped through a metal capillary which is held at high voltage.

In order to cope with small volumes of liquid solution, miniaturized ESI ion sources with low flow rates have also been developed using pulled glass capillaries.^{6–9} Wilm and Mann described theoretically and demonstrated experimentally that a narrower spraying capillary with a much reduced flow rate could generate smaller initial droplets, and hence better ion desorption from the liquid.⁸ Derived from its nanoliter flow rates, the technique is now widely referred to as nanoelectrospray (nanoESI), and it has been shown to work with high-polarity solvents such as pure water,¹⁰ and to tolerate higher concentrations of buffer salts than conventional ESI.^{9,11}

Due to the smaller aperture size of the capillary, needle clogging may occur during the analysis, and to reopen the plugged capillaries, the tip is usually touched against the counter electrode to break it up. As a consequence, the reproducibility of ion intensity may vary due to the difference in the final tip diameter, even though identical nanoESI needles are used initially.¹² In addition to clogging, it may also be difficult to

initiate the electrospray from capillaries with diameters smaller than 1 μm due to the surface tension of the liquid.

Several designs of electrospray ion sources that use noncapillary probes had been put forward to overcome the clogging problem. Shiea et al. succeeded in electrospaying a sample solution deposited on a copper wire ring after applying a high voltage to the copper wire, and mass spectra of proteins similar to those of conventional ESI could also be obtained.¹³ The technique was further explored using optical fibers wired with copper or platinum wires,^{14,15} a glass rod,¹⁶ and nanostructured tungsten oxide.¹⁷ Electrospray from the solution deposited on micropillar chips has also been reported.¹⁸

Recently, a probe electrospray ionization (PESI) method using a sharp solid needle as the electrospray emitter has been developed in our laboratory.¹⁹ The stainless steel needle was repeatedly loaded with a small amount of sample solution by touching the liquid surface with a needle tip, and the electrospray could be generated when high voltage (HV) was applied to the needle. Neither nebulizing gas nor a sheath liquid was needed, and ion signals for amino acids, peptides, and proteins could be detected even from a single sample loading. The method is free of clogging problems, and could be used to analyze real-world biological samples directly without any sample preparations.²⁰ In this paper, we report the analytical characteristics of probe electrospray based on the measurement of spray current, pulsed laser microscopy, and PESI mass spectrometry (PESI-MS).

Experimental Section

PESI Ion Source. PESI-MS experiments were performed on an orthogonal-acceleration time-of-flight mass spectrometer (AccuTOF, JEOL, Akishima, Japan). The original electrospray ion source was removed to accommodate the PESI ion source. The configuration of the ion source was similar to that which has been illustrated in our previous report.¹⁹

* Corresponding author. E-mail: hiraoka@yamanashi.ac.jp.

[†] Clean Energy Research Center.

[‡] Department of Anatomy and Cell Biology.

[§] Department of Epigenetic Medicine.

^{||} Interdisciplinary Graduate School of Medicine and Engineering.

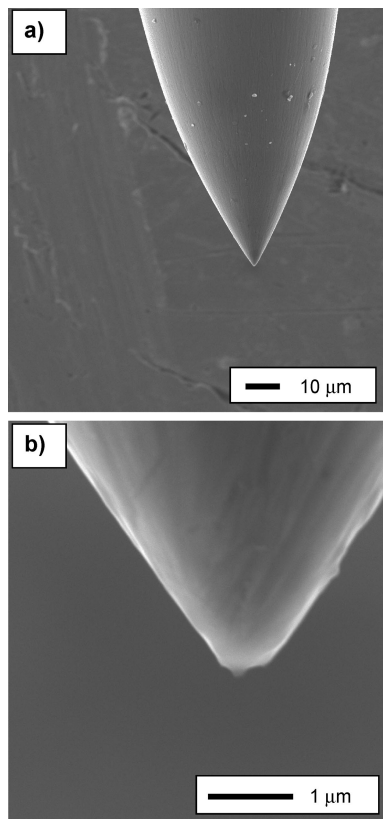


Figure 1. (a) Scanning electron micrograph of the solid needle probe used in the PESI-MS experiment. (b) Close-up of the tip of the needle.

In brief, the needle was aligned vertically at an angle orthogonal to the axis of the ion-sampling orifice. The needle was moved up and down the vertical axis, and when the needle was at the highest position, the vertical and horizontal distances from the apex of the ion-sampling orifice were 2–3 and 3–5 mm, respectively. The sample reservoir was mounted on a stage placed below the sampling orifice and was adjusted in such a way that the tip of the needle touched the liquid surface when the needle was moved down to the lowest position. A small amount of sample could be repeatedly reloaded to the needle by driving the needle with a linear actuator, or motor-driven system. In this study, we used a linear actuator system equipped with two limit sensors at the highest and lowest positions (ARIOS, Akishima, Tokyo, Japan). The needle was actuated at the frequency of ~ 3 Hz with the moving stroke of 8–10 mm.

Disposable acupuncture needles (Seirin, Shizuoka, Japan) with submicrometer tip diameters were used as electrospray emitters throughout the PESI-MS experiment. The sterilized needles were hermetically sealed when purchased and could be used directly without any further washing. The shapes and sizes of the needles were inspected using a scanning electron microscope (SEM) as shown in Figure 1. The geometric shapes of the needles were found to be almost identical, and all were of submicrometer size.

High voltage could be applied to the needle using several methods. When the sample stage was grounded, the high voltage was applied using an HV amplifier which was controlled by position sensors (e.g., ground potential at the lowest position and HV at the highest position). When the sample was electrically floated or held at HV, constant high voltage from a regulated HV supply could be applied directly to the needle. In this case, as the needle was moved close to the sampling orifice,

electrospray would be initiated once a sufficient electric field was established. Depending on the condition of needle alignment and the types of analyte, the applied HV was in the range of 2–3 kV.

Measurement of Spray Current. The electrospray current flowing through the needle (typically in the range of tens of nanoamperes) was measured by connecting a shunt resistor (2 k Ω) in series with the needle at the high-voltage side. The voltage drop across the resistor was amplified accordingly using a precision amplifier, and was coupled to the low-voltage side by using two cascaded isolation amplifiers (ISO 124P, Texas Instruments, USA). The current signal was monitored during the PESI-MS measurement using a digital oscilloscope (TDS 5054B, Tektronics, USA).

Optical Microscopy of Electrospray from Solid Needle Probe. The tip of the solid needle was illuminated using a frequency-doubled Nd:YAG pulsed laser (532 nm wavelength) with the pulse width of 4 ns, and the electrospray generated from the tip was observed using a long working-distance lens. The focused laser beam was aligned to be slightly away from the needle tip, and we assumed negligible optical absorption of liquid sample at this laser wavelength. The pulsing of the laser was synchronized with the needle motion using a pulse delay generator (Stanford Research, USA). The forward scattering light from the electrosprayed droplets was captured using a digital camera (Canon EOS, 10 million pixels), and the camera shutter was controlled in such a way that only one laser shot was recorded in each capture. The captured images were processed using GIMP (a GNU open source program).

Sample Preparation. Gramicidin S, bovine insulin, and acetic acid were purchased from SIGMA (Sigma-Aldrich, USA), and bradykinin was from Calbiochem. Solvents and buffer solution were of reagent grade, and all chemicals were used without further purification. Pure water was prepared using a Milli-Q system (Millipore, USA). Insulin was prepared in 10^{-5} M in 1% acetic acid aqueous solution. Gramicidin S and bradykinin were prepared in a concentration of $\sim 10^{-5}$ M in 10^{-2} M ammonium acetate or in 0.1% acetic acid aqueous solution.

Results and Discussion

In conventional electrospray or nanoelectrospray that uses capillary needles, the aperture size of the capillary determines the size of the Taylor cone, flow rate, and hence the initial diameter of the sprayed droplet. In analogy, for probe electrospray where sample solution is electrosprayed from a solid needle, the tip diameter is one of the important factors that determine the spraying condition.

Parts d, e, and f of Figure 2 show snapshots of the electrospray generated from three solid needles, with tip diameters of <1 , ~ 10 , and ~ 100 μm , respectively. Backlight illumination photographs for these needles are shown respectively in parts a, b, and c of Figure 2. The liquid sample was 10^{-5} M gramicidin S in 10^{-2} M ammonium acetate aqueous solution, and the needle was flashed with the pulsed laser (pulse width, 4 ns) at several tens of milliseconds after the application of high voltage.

For comparison, the electrospraying of 0.1% acetic acid in water/methanol ($v/v = 1/1$) using a nanoelectrospray capillary (i.d. ~ 5 μm , SilicaTips from New Objective), and a conventional electrospray capillary (i.d. ~ 100 μm , liquid flow rate ~ 1 $\mu\text{L}/\text{min}$ without nebulizing gas) are shown respectively in Figure 2g and 2h. The capillary needles were held at 1–1.5 kV for nanoESI and 3–3.7 kV for ESI, and the distance between the needle and the counter electrode was 5–10 mm.

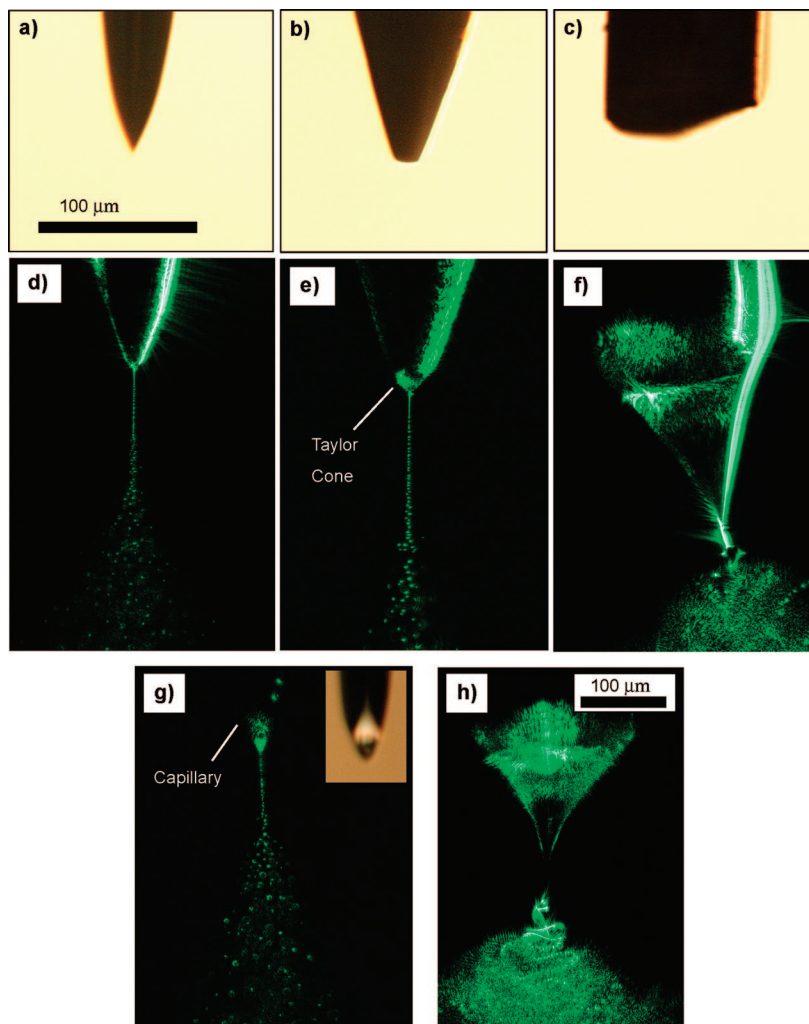


Figure 2. Backlight illumination photographs and electrospray images captured using pulsed laser microscopy for (a, d) solid needle of $<1\ \mu\text{m}$ tip diameter, (b, e) solid needle of $\sim 10\ \mu\text{m}$ tip diameter, and (c, f) blunted solid needle of $\sim 100\ \mu\text{m}$ in diameter. (g) Image for nanoelectrospray from capillary of $\sim 5\ \mu\text{m}$ inner diameter; the shape of the capillary is shown in the inset with the same magnification. (h) Conventional electrospray generated using capillary of $\sim 100\ \mu\text{m}$ inner diameter. The scale bar in (a) is also valid for (b)–(g).

As depicted in Figure 2d, a small droplet of sample solution of $\sim 1\ \mu\text{m}$ in diameter was formed on the tip of the needle, possibly in the shape of a Taylor cone, and fine charged droplets were electrosprayed from the cusp, similar to that of capillary nanoelectrospray shown in Figure 2g. Owing to the very short laser illumination time (4 ns), sprayed droplets appeared to be at a total standstill, and the scattered light from a single charged droplet can also be identified easily. However, it should be noted that, due to the diffraction limit of the optical microscopy, the exact size of the sprayed droplet cannot be determined from these images. As the solvent evaporated, the scattered-light spot appeared to be bigger when it was further from the tip. There was also some scattering light from the body of the solid needle which was not related to the electrospray.

For the solid needle with the tip diameter of $\sim 10\ \mu\text{m}$ shown in Figure 2b,e, the liquid Taylor cone formed on the tip was apparently bigger, with the base diameter of the cone similar to the size of the needle tip. For the blunted solid needle in Figure 2c, higher HV was needed to initiate the electrospray, and the spraying condition became similar to conventional electrospray that used a capillary of $\sim 100\ \mu\text{m}$ inner diameter. Unless otherwise stated, medical acupuncture needles of $<1\ \mu\text{m}$ tip diameter were used in the following measurements.

To visualize the formation of the electrospray from the solid needle, time-lapse images of the needle tip after the application

of high voltage were obtained using a pulsed laser. In order to maintain the needle position for every record, the experimental condition was slightly modified from that of the PESI-MS in such a way that the liquid solution was fed to the needle by moving the sample stage at $\sim 3.3\ \text{Hz}$ while keeping the needle stationary. The liquid sample was $10^{-5}\ \text{M}$ gramicidin S in $10^{-2}\ \text{M}$ ammonium acetate aqueous solution, and the high voltage was applied to the needle for a duration of 100 ms using an HV amplifier. The tip of the needle was illuminated with the pulsed Nd:YAG laser at different delay times after the application of the HV, and only one image was captured for one sampling cycle. In order to identify the spray more clearly, the captured images were color-inverted and were converted to gray scale (e.g., the region with bright scattered light will appear dark and vice versa).

Since no external pump is used in PESI, it relies on the electrostatic force acting on the liquid film to deliver the sample toward the tip to produce stable electrospray. As shown in Figure 3, liquid accumulation (as indicated by a small dark spot) was found on the needle tip at $\sim 1\ \text{ms}$ after the application of high voltage. The electrospray emission from the accumulated solution becomes observable at about 5 ms. The intensity of the scattered light increases with the delay time due to the increase of flow rate and the amount of sprayed droplet, and decreases gradually with the consumption of liquid sample.

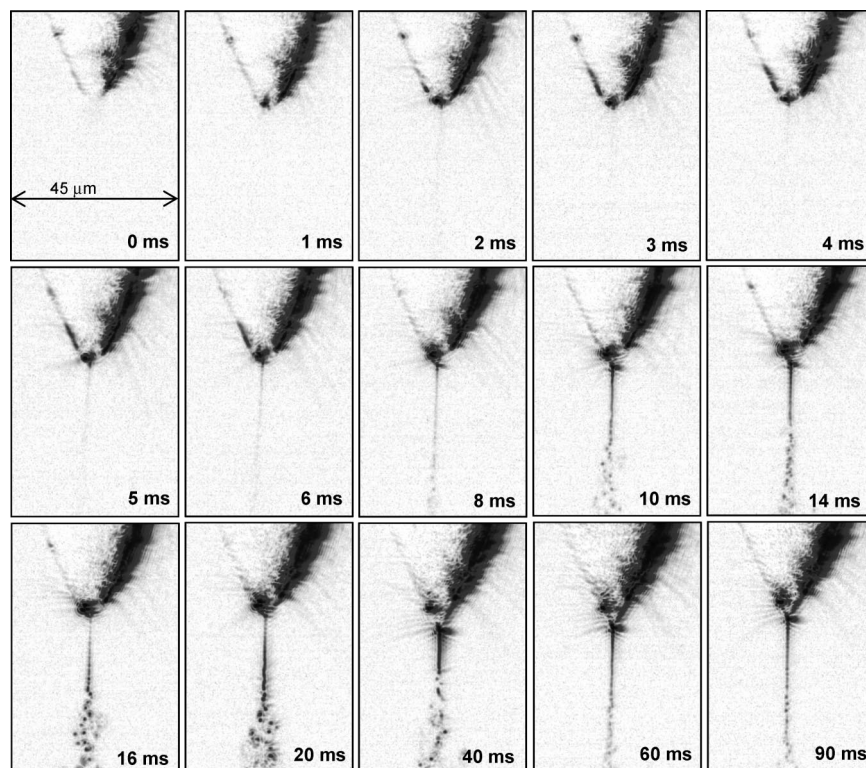


Figure 3. Time-lapse images on the formation of electrospray from the solid needle probe. The needle tip was illuminated with a pulsed laser (pulse width, 4 ns) at a delay time measured from the application of high voltage. The liquid sample is 10^{-5} M gramicidin S in 10^{-2} M ammonium acetate aqueous solution.

The spray current in capillary ESI is of interest due to its dependence on the liquid flow rate.^{21,22} In our experiment, the current flowing through the solid needle was measured simultaneously with the PESI-MS measurement. The amount of liquid picked up by the needle depends on the dipping depth, and the temporal spray currents for different dipping depths into the aqueous solution of 10^{-5} M gramicidin S and 10^{-2} M ammonium acetate are shown in Figure 4. In this measurement, the solid needle was held at a constant voltage of 2.5 kV, and the liquid sample was kept in a plastic microtube which was electrically insulated from the ground.

The illustrated needle motion in Figure 4 was derived from the outputs of two limit sensors that sense the needle at the highest and lowest positions. The sample stage was first adjusted to a position where the needle tip just touched the liquid surface with detectable spray current, and this initial depth is denoted as d_0 . At $d_0 - 0.1$ mm, the needle was in no contact with the liquid sample and no spray current was detected. The exact value for d_0 is not known but is estimated to be about 0.1 mm or less. Asterisks (*) in Figures 4, 5, and 6 denote the electrical noise when the needle tip moved across the ion-sampling orifice of the mass spectrometer.

As the needle moved upward, electrospray was initiated spontaneously at a certain needle position when sufficient electric field was established at the needle tip. For a small amount of liquid (d_0 to $d_0 + 0.5$ mm), the spray current rose to a peak value and decreased gradually due to the consumption of liquid sample, with its width in each sampling cycle dependent on the dipping depth. For a larger dipping depth such as that in $d_0 + 0.8$ mm, the liquid amount loaded to the tip was enough to sustain a stable electrospray (constant flow rate) for a short period of time before the sample was totally consumed. In the case of $d_0 + 1.2$ mm, the loaded liquid could not be completely sprayed within the designated period, and was

quenched when the needle moved downward for the next sampling process. When the needle was overloaded with liquid sample, e.g., at the dipping depth of $d_0 + 2$ mm, the current oscillated in the range of kilohertz to tens of kilohertz. This current fluctuation is likely to be related to the spontaneous spray pulsation which is known to exist in most conventional electrosprays.^{23–25}

Although the peak spray current changed slightly with the amount of loaded sample, it was more dependent on the applied voltage, as shown in Figure 5. At the same dipping depth (~ 0.1 mm) into the sample of 10^{-5} M gramicidin S and 10^{-2} M ammonium acetate aqueous solution, the liquid flow rate, as indicated by the spray currents, increased significantly with the applied voltage and the liquid sample was consumed in a rather shorter time with higher applied voltage.

On certain occasions, depending on the analyte and the ambient condition, increasing the applied voltages could easily induce a drastic increase of discharge current when the electrospray was almost complete due to the gas breakdown. Figure 6 shows the needle currents at different applied voltages for the electrospray of 10^{-6} M gramicidin S in 0.1% acetic acid aqueous solution. With the applied voltage increased to ≥ 2.5 kV, the appearance of discharge current besides the spray current indicates the occurrence of gas-phase breakdown. The gas breakdown could be suppressed to a certain extent by increasing the liquid amount or moving the needle at higher frequency. However, in the following PESI-MS measurement, the applied voltage was simply adjusted to not exceed the discharge current threshold.

The influence of applied voltage on the PESI-MS is shown by the mass spectra of bradykinin and gramicidin S mixture in Figure 7. The aqueous solution (0.1% acetic acid in pure water) contained bradykinin and gramicidin S in the concentrations of $\sim 3 \times 10^{-5}$ M and $\sim 1 \times 10^{-5}$ M, respectively. At 2.0 kV (peak

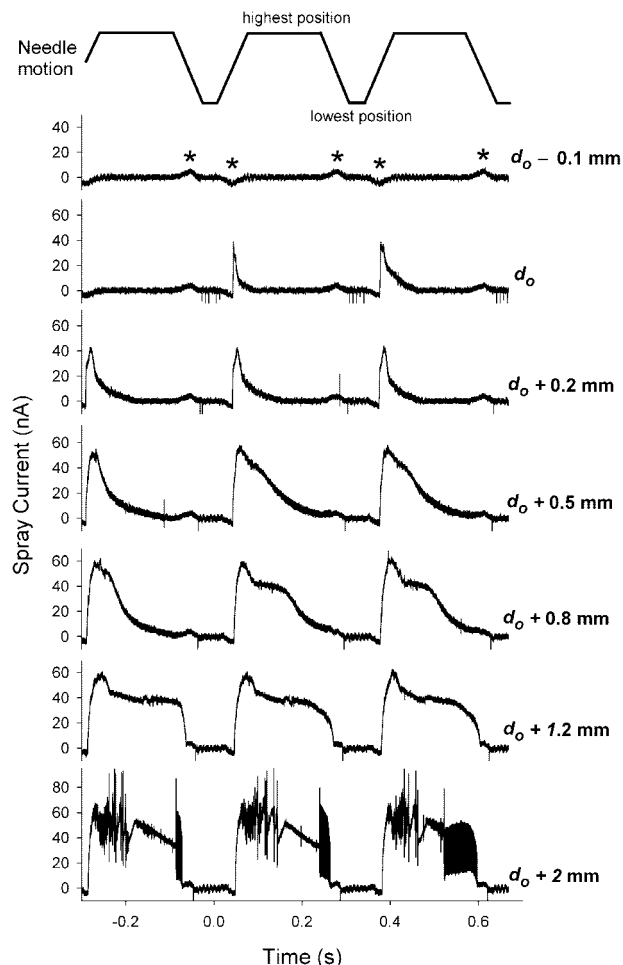


Figure 4. Spray current for different dipping depths of the needle into 10^{-5} M gramicidin S and 10^{-2} M ammonium acetate aqueous solution. The solid needle is held at 2.5 kV, and d_o denotes the dipping depth where the needle tip just touched the liquid surface with detectable spray current. The exact position of d_o is not known but is estimated to be $\sim 100 \mu\text{m}$ or less. Asterisks (*) denote the electrical noise when the needle moved across the ion-sampling orifice of the mass spectrometer.

spray current ~ 20 nA, the ion signal for $[\text{bradykinin} + 2\text{H}]^{2+}$ was much weaker than that of $[\text{gramicidin S} + 2\text{H}]^{2+}$, and $[\text{bradykinin} + \text{H}]^+$ was barely detected. The ion signal for $[\text{bradykinin} + 2\text{H}]^{2+}$ increased with the applied voltage, and at 2.6 kV (peak spray current about 50–60 nA), the ion abundance of $[\text{bradykinin} + 2\text{H}]^{2+}$ became equal to or greater than that of $[\text{gramicidin S} + 2\text{H}]^{2+}$. As gramicidin S is more surface active than the relatively hydrophilic bradykinin,²⁶ the results in Figure 7 are likely related to the analyte surface activities.

Analyte surface activities have been known to affect conventional ESI-MS so that the more surface-active (more hydrophobic) analyte ions will be enriched on the sprayed droplet surface, making the desorption and detection of these ions easier.²⁷ The ions of the relatively hydrophilic analyte would however be suppressed by this surface-activity effect. In capillary ESI, Wilm and Mann postulated that such ion suppression could be overcome by nanoelectrospray owing to the formation of smaller initial charged droplets.^{8,9} Similarly, the reduced ion suppression of bradykinin in Figure 7c was possibly due to the finer initial droplets generated at higher applied voltage.

Besides the charged droplet surface, the surface-active analyte could also be enriched on the liquid meniscus surface before

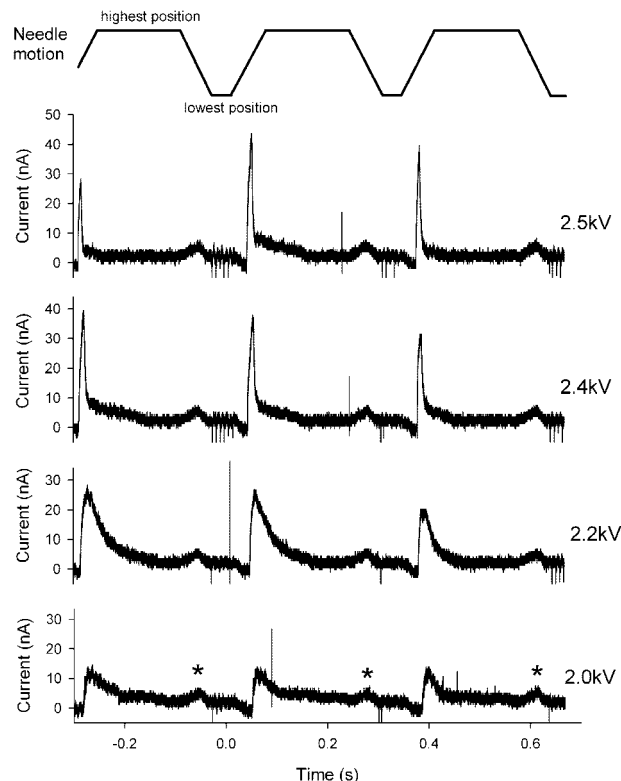


Figure 5. Needle current at different applied voltages for electro-spraying of 10^{-5} M gramicidin S in 10^{-2} M ammonium acetate aqueous solution. The dipping depth was kept at ~ 0.1 mm. Asterisks (*) denote the electrical noise when the needle moved across the ion-sampling orifice.

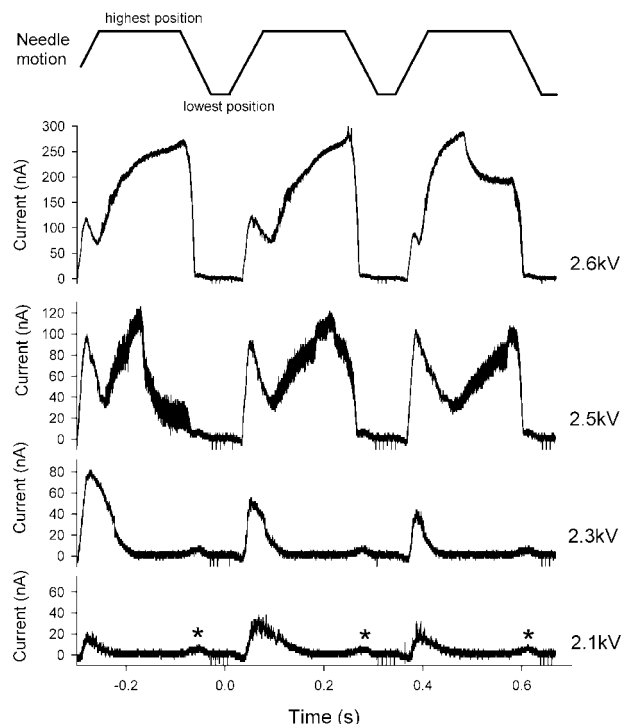


Figure 6. Needle current at different applied voltages for the electro-spray of 10^{-6} M gramicidin S in 0.1% acetic acid aqueous solution. The voltage was increased until the appearance of discharge current.

being electrosprayed. Thus it is also possible that the surface-active analyte was preferentially sprayed at lower applied voltage (as in Figure 7a) and some of the relatively hydrophilic analyte

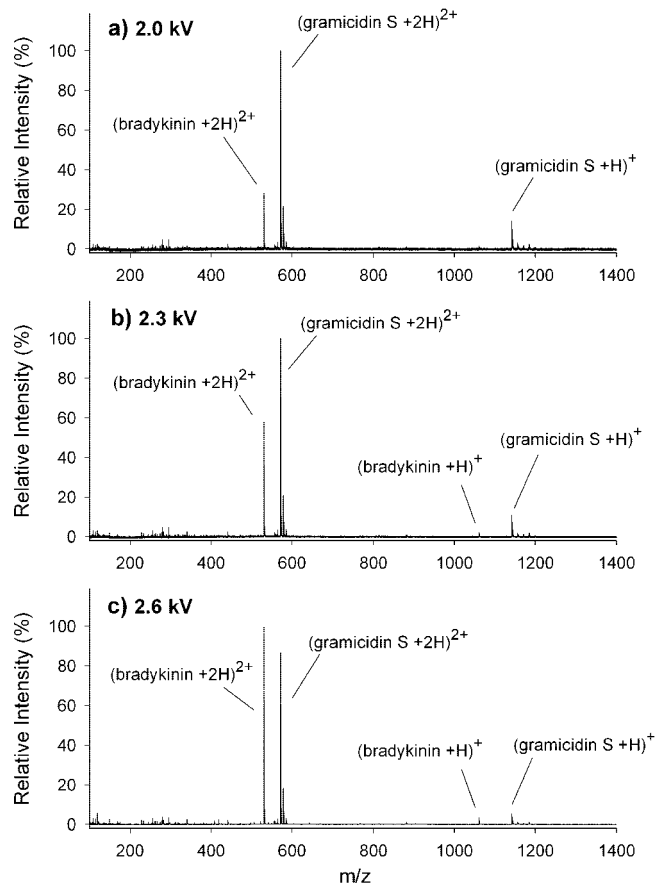


Figure 7. PESI mass spectra for a solution of $\sim 3 \times 10^{-5}$ M bradykinin and $\sim 1 \times 10^{-5}$ M gramicidin S in 0.1% acetic acid aqueous solution at different applied voltages.

was left on the tip after the liquid surface tension could no longer be overcome by the electric field.

Optimizing the voltage applied to the needle could also have a pronounced effect on the analyte solution containing salt contaminants. Figure 8 shows the dependence of PESI mass spectra on the applied voltage for bovine insulin (10^{-5} M) in 1% acetic acid and 10 mM NaCl aqueous solution. The mass spectrum obtained at 2.4 kV (peak current ~ 150 nA), and the expanded mass spectrum for charge state 4+ are shown in Figure 8a and Figure 8b, respectively. With the addition of salt, the spray current increased considerably due to the increase in liquid conductivity. Insulin was detected in the charge states of 3+ to 6+, with some sodium adducts for the lower charge states (e.g., 3+ and 4+). The adduct ion formation could however be suppressed by reducing the liquid flow rate, that is by decreasing the applied voltage as shown in Figure 8c (2.0 kV applied voltage, peak current ~ 70 nA). This result is in agreement with that of the nanoESI-MS, where sodium adducts could be reduced by further reducing the liquid flow rate.¹² However, as the liquid flow rate can only be controlled by the applied voltage to a certain extent in the present PESI experiment, further reduction in flow rate should involve the use of needles of an even smaller size, which is currently underway in our laboratory.

Conclusion

We have shown that by using a solid needle with a small tip diameter, a fine electrospray jet could be produced from the tiny liquid droplet formed on the needle tip, with the spraying condition quite similar to that of nanoESI. PESI also shares the advantages of nanoESI in low sample consumption, and higher

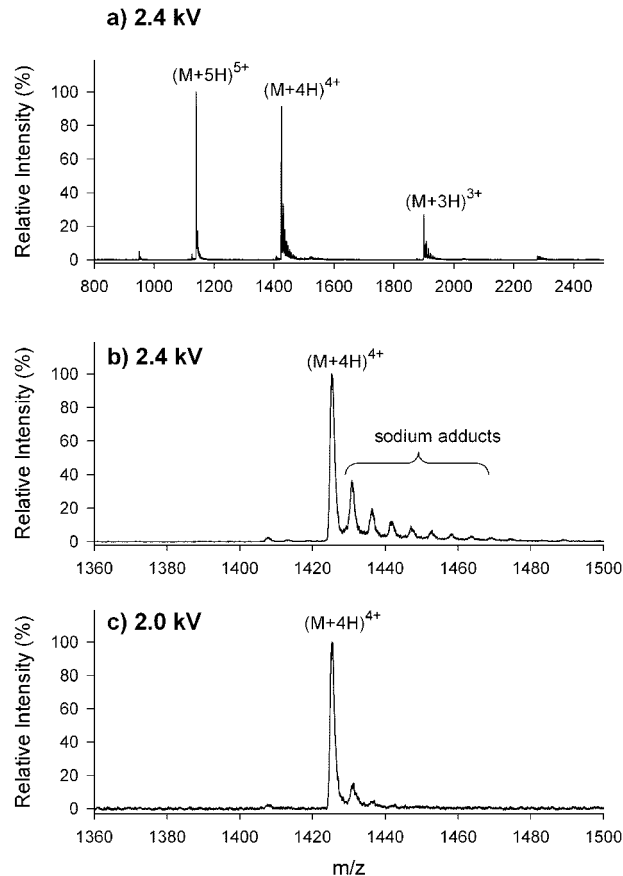


Figure 8. PESI mass spectra for 10^{-5} M bovine insulin in 0.1% acetic acid aqueous solution. (a) Mass spectrum acquired at 2.4 kV. (b) Expanded mass spectrum for charge state 4+ in (a). (c) Mass spectrum for charge state 4+ obtained at 2.0 kV.

tolerability to salt buffer compared to conventional ESI. As monitored by the spray current, a small amount of liquid sample could be thoroughly and reproducibly electrosprayed for every sampling cycle. As no external pump is used in PESI, the liquid flow rate depends on the voltage applied to the needle as well as the liquid amount loaded on the probe tip. The effects of applied voltage and the liquid flow rate on the PESI mass spectra have also been demonstrated.

Under the present experimental conditions, the threshold voltage for the onset of electrospray is in the range of 2 kV, which is higher than that of the nanoelectrospray, and this may be due to the following aspects: (1) Although the solid needle has a submicrometer tip diameter, the root diameter is around $100 \mu\text{m}$ and it is tapered at a rather low aspect ratio; hence the electric field at a given voltage²⁸ may be lower than that of metal coated nanoESI capillaries, which usually have higher aspect ratios. (2) The solid needle is used without any surface modification, and when the liquid is loaded to a region away from the tip, higher applied voltage is also needed to deliver the liquid to the tip for the onset of electrospray.

Further improvements on PESI thus include the optimization on the shape of the solid needle, and the chemical modification on the needle surface so that only the tip with desirable surface area is to be wet with the liquid sample. By further downsizing the solid needle tip, PESI may offer a possibility of producing even finer droplets than that of nanoESI, and it would be interesting to explore if gaseous molecular ions could be emitted directly from the wetted needle tip of much smaller size and higher curvature.

Acknowledgment. This work is supported by the Development of System and Technology for Advanced Measurement and Analysis Program (SENTAN) from the Japan Science and Technology Agency.

References and Notes

- (1) Zeleny, J. *Phys. Rev.* **1917**, *10*, 1.
- (2) Taylor, G. *Proc. R. Soc. London, Ser. A* **1964**, *280*, 383.
- (3) Dole, M.; Mack, L. L.; Hines, R. L.; Mobley, R. C.; Ferguson, L. D.; Alice, M. B. *J. Chem. Phys.* **1968**, *49*, 2240.
- (4) Yamashita, M.; Fenn, J. B. *J. Phys. Chem.* **1984**, *88*, 4451.
- (5) Fenn, J. B.; Mann, M.; Meng, C. K.; Wong, S. F.; Whitehouse, C. M. *Science* **1989**, *246*, 64.
- (6) Wahl, J. H.; Goodlett, D. R.; Udseth, H. R.; Smith, R. D. *Anal. Chem.* **1992**, *64*, 3194.
- (7) Emmett, M. R.; Caprioli, R. M. *J. Am. Soc. Mass Spectrom.* **1994**, *5*, 605.
- (8) Wilm, M. S.; Mann, M. *Int. J. Mass Spectrom. Ion Processes* **1994**, *136*, 167.
- (9) Wilm, M.; Mann, M. *Anal. Chem.* **1996**, *68*, 1.
- (10) Wilm, M.; Shevchenko, A.; Houthaeve, T.; Breit, S.; Schweigerer, L.; Fotsis, T.; Mann, M. *Nature* **1996**, *379*, 466.
- (11) Juraschek, R.; Dülcks, T.; Karas, M. *J. Am. Soc. Mass Spectrom.* **1999**, *10*, 300.
- (12) Schmidt, A.; Karas, M.; Dülcks, T. *J. Am. Soc. Mass Spectrom.* **2003**, *14*, 492.
- (13) Hong, C.-M.; Lee, C.-T.; Lee, Y.-M.; Kuo, C.-P.; Yuan, C.-H.; Shiea, J. *Rapid Commun. Mass Spectrom.* **1999**, *13*, 21.
- (14) Kuo, C.-P.; Shiea, J. *Anal. Chem.* **1999**, *71*, 4413.
- (15) Kuo, C.-P.; Yuan, C.-H.; Shiea, J. *J. Am. Soc. Mass Spectrom.* **2000**, *11*, 464.
- (16) Jeng, J.; Shiea, J. *Rapid Commun. Mass Spectrom.* **2003**, *17*, 1709.
- (17) Jeng, J.; Lin, C.-H.; Shiea, J. *Anal. Chem.* **2005**, *77*, 8170.
- (18) Nissilä, T.; Sainiemi, L.; Sikanen, T.; Kotiaho, T.; Franssila, S.; Kostiaainen, R.; Ketola, R. A. *Rapid Commun. Mass Spectrom.* **2007**, *21*, 3677.
- (19) Hiraoka, K.; Nishidate, K.; Mori, K.; Asakawa, D.; Suzuki, S. *Rapid Commun. Mass Spectrom.* **2007**, *21*, 3139.
- (20) Chen, L. C.; Nishidate, K.; Saito, Y.; Mori, K.; Asakawa, D.; Takeda, S.; Kubota, T.; Terada, N.; Hashimoto, Y.; Hori, H.; Hiraoka, K. *Rapid Commun. Mass Spectrom.* **2008**, *22*, 2366.
- (21) Pfeifer, R. J.; Hendrick, C. D. *AIAA J.* **1968**, *6*, 496.
- (22) Fernandez de la Mora, J.; Loscertales, I. G. *J. Fluid Mech.* **1994**, *260*, 155.
- (23) Juraschek, R.; Röllgen, F. W. *Int. J. Mass Spectrom.* **1998**, *177*, 1.
- (24) Wei, J.; Shui, W.; Zhou, F.; Lu, Y.; Chen, K.; Xu, G.; Yang, P. *Mass Spectrom. Rev.* **2002**, *21*, 148.
- (25) Marginean, I.; Parvin, L.; Heffernan, L.; Vertes, A. *Anal. Chem.* **2004**, *76*, 4202.
- (26) Hiraoka, K.; Mori, K.; Asakawa, D. *J. Mass Spectrom.* **2006**, *41*, 894.
- (27) Kebarle, P. *J. Mass Spectrom.* **2000**, *35*, 804.
- (28) Smith, R. C.; Carey, J. D.; Forrest, R. D.; Silva, S. R. P. *J. Vac. Sci. Technol., B* **2005**, *23*, 632.

JP803730X